Article

Not peer-reviewed version

Collision Frequency and Energy Transfer Rate in e-He Scattering

Yeldos Seitkozhanov *, Karlygash Dzhumagulova *, Erik Shalenov, Murat Jumagulov

Posted Date: 20 November 2024

doi: 10.20944/preprints202411.1356.v1

Keywords: plasma physics; collision frequency; energy transfer rate; electron scattering; optical potential; phase function method

 doi:10.20944/preprints202411.1356.v1

Article

Collision Frequency and Energy Transfer Rate in e-He Scattering

Yeldos Seitkozhanov [1,2,*], Karlygash Dzhumagulova [1,2,3,*], Erik Shalenov [1] and Murat Jumagulov [1]

[1] Department of General Physics, Satbayev University, Almaty 050013, Kazakhstan
[2] Department of Plasma Physics, Nanotechnology and Computer Physics, Al-Farabi Kazakh National University, Almaty 050040, Kazakhstan
[3] Institute of Experimental and Theoretical Physics, Al-Farabi Kazakh National University, Almaty 050040, Kazakhstan
* Correspondence: seytkozhanov@gmail.com (Y.S.); dzhumagulova.karlygash@gmail.com (K.D.)

Abstract: Using the optical interaction potential between an electron and a helium atom, we calculate the collision frequency and energy transfer rate during the elastic scattering of electrons on helium atoms. The resulting effective frequency as a function of energy exhibits a maximum consistent with experimental data. The rate of energy transfer is in good agreement with other authors' calculations at low electron energies, with discrepancies increasing as the energy increases.

Keywords: plasma physics; collision frequency; energy transfer rate; electron scattering; optical potential; phase function method

1. Introduction

For the successful development of plasma technologies, accurate data on the properties of the generated plasma and the processes occurring within it are necessary. Such data can be obtained and interpreted through experimental and theoretical studies that complement each other. It should be noted that particle collisions involving free electrons play a key role in plasma processes. Over the past few decades, significant progress has been made in computational and experimental methods used to study and simulate electron-driven processes. The advent of modern supercomputers has made it possible to model collisions involving electrons and complex atomic or molecular systems, significantly enhancing the ability to simulate and analyze the behavior of various plasmas [1–4].

Electron collision physics finds applications across numerous fields, including thermonuclear fusion research [5–8], atmospheric and space sciences [9,10], radiation physics [11–13], semiconductor technology [14–16], and medical diagnostics [17–19], where understanding electron interactions with atoms and molecules is crucial for both experimental and theoretical advancements. In connection with the urgent problems of energy supply in the modern world, a very important area is the study of the properties of plasma generated in controlled thermonuclear fusion plants with magnetic confinement. In the divertor region of tokamak-type installations, bound states, specifically helium atoms, are present alongside charged electrons and ions. This study investigates some physical quantities caused by electron scattering on helium atoms in tokamak plasma, including collision frequencies and energy transfer rates.

As is well known, particle collisions establish temperature equilibrium in a multi-particle system. In the case of plasma, a critical task is determining the temperatures of its various components. To accomplish this, energy balance equations can be used, requiring data on energy transfer rates between colliding particles [20–24]. A general expression for the average energy exchange rate between two gases with a Maxwellian velocity distribution in thermal disequilibrium was obtained by Desloge [25]. Banks [22] used this expression to calculate collision frequencies and energy transfer rates of interest in aeronomy. Itikawa [26] showed that the average collision frequency for energy transfer, as determined by Banks, gives satisfactory results when used to calculate transfer coefficients. However, he found that some of Banks' semi-empirical collision frequency formulas are inaccurate at high electron temperatures.

 doi:10.20944/preprints202411.1356.v1

The formalism describing the energy transfer rate, by defining an appropriate collision frequency and momentum-transfer cross section was developed by Banks, who originally applied it in aeronomy in the upper atmosphere [22]. In the framework of this formalism, the cross-section of electron-atom collisions was taken as a constant value. Banks' approach remains relevant for the divertor region of the tokamaks at relatively low energies (up to several eV). In our work, we determine the cross-section of electron-atom collisions based on the phase function method, which gives us the dependence of the cross-section on the energy of the incident particle and ultimately affects the collision frequency and the rate of energy transfer in electron-atom collisions.

An important point is also the question of the influence of the plasma environment on collision processes in the divertor region of the tokamak. It is well known that in the central region of the tokamak and in the divertor region, which is not adjacent to the walls, the plasma is almost ideal in the sense that the kinetic energy of the plasma particles greatly exceeds the potential energy of particle interaction at the average interparticle distance. The parameter characterizing the non-ideality of the plasma is the coupling parameter:

$$\Gamma = \frac{e^2}{4\pi\epsilon_0 a k_B T}. \tag{1}$$

where e is the elementary charge, ϵ_0 is the permittivity of free space, k_B is the Boltzmann constant, $a = \left(\frac{3}{4\pi n}\right)^{1/3}$, n is the plasma density and T is the temperature of the plasma. For ideal plasma, $\Gamma \ll 1$. Even though in the divertor region the electron density is higher compared to the upper atmosphere, nevertheless the coupling parameter remains low, i.e., $\Gamma \ll 1$. This indicates that in this system the influence of collective effects can be neglected. Thus, electron-atom collisions in the divertor region, as well as in the upper atmosphere, are treated as two-body interactions with negligible screening effects of the plasma environment.

The structure of this paper is as follows: Section 2 provides a detailed explanation of the methods used in calculating the collision frequency and energy transfer rate for electron-helium scattering. Section 3 presents the results of implementing the above methods. The final part contains conclusions.

2. Methods

2.1. Momentum-Transfer Cross-Sections via the Method of Phase Functions

To accurately determine the collision frequency and energy transfer rate in particle interactions, it is essential to calculate the momentum transfer cross-section, which represents the average momentum transferred by a particle during a collision. This cross-section is calculated using the partial wave decomposition of scattered waves:

$$Q_T^{ea}(k) = \frac{4\pi}{k^2} \sum_{l=0}^{\infty} (l+1) \sin^2(\delta_{l+1} - \delta_l). \tag{2}$$

To perform this calculation, we employed the method of phase functions [27], also known as the variable phase approach [28]. This technique efficiently computes the phase shifts δ_l, by solving the first-degree phase equation, thereby circumventing the exhaustive wave function calculations typical of conventional approaches [29,30]. The interaction potential used in the phase equation is defined via the optical potential approach, as detailed in the following section.

The phase equation is given as follows:

$$\frac{d\delta_l(r)}{dr} = -\frac{1}{k}\left(\frac{2m_e}{\hbar^2}\right) V(r)[\cos(\delta_l(r)) j_l(kr) - \sin(\delta_l(r)) n_l(kr)]^2, \tag{3}$$

and is solved with the boundary condition:

$$\delta_l(0) = 0, \tag{4}$$

 doi:10.20944/preprints202411.1356.v1

where $\delta_l(r)$ is the phase function, $V(r)$ is the interaction potential between an electron and an atom at a distance r from the atomic nucleus, $j_l(kr)$ and $n_l(kr)$ are the Riccati-Bessel functions, k is the wave number of the incoming electron, m_e is the electron mass, and $\hbar$ is the reduced Planck's constant. The phase shift is defined as the asymptotic value of the phase function at large distances:

$$\delta_l = \lim_{r\to\infty} \delta_l(r). \tag{5}$$

2.2. Optical Potential

At relatively low energies, the study of electron scattering on atoms becomes increasingly complex due to the necessity of accounting for multiparticle interactions. To address this challenge, the optical potential method simplifies the analysis by reducing electron scattering to a consideration of the pair interaction potential $V_{\text{opt}}(r)$. This potential can be expressed as a sum of three key components: static, correlation-polarization, and exchange interactions:

$$V_{\text{opt}}(r) = V_S(r) + V_P(r) + V_{\text{ex}}(r). \tag{6}$$

The static potential $V_S(r)$ represents the Coulomb interaction between an electron and the nucleus, as well as the other electrons of the target atom, characterized by its electron density $\rho(r)$ and charge number Z. When the electron density at position r', denoted as $\rho(r')$, is derived by solving the Schrödinger equation, the potential is referred to as the Hartree-Fock potential:

$$V_{HF}(r) = -\frac{Ze^2}{4\pi\epsilon_0 r} + \frac{e^2}{4\pi\epsilon_0}\int \frac{\rho(r')}{|r-r'|} d^3r'. \tag{7}$$

In scenarios where relativistic effects are significant, the Dirac equation can be employed, resulting in the Dirac-Hartree-Fock-Slater potential $V_{DHFS}(r)$. For our analysis, we utilized the analytical form of the static potential $V_{DHFS}(r)$ as presented by Salvat et al. [31]:

$$V_{DHFS}(r) = -\frac{Z}{r}\sum_{i=1}^{N} A_i e^{-\alpha_i r}, \tag{8}$$

where A_i and α_i are fitting parameters specific to the target atom, with their values for helium provided in Table 1.

Table 1. Parameters for Helium.

Z	A_1	A_2	α_1	α_2
2	-0.2259	1.2259	5.5272	2.3992

The incoming electrons induce a polarization of the charge cloud of the target atom, which leads to an induced dipole moment that, in turn, acts back on the electrons. The semi-empirical potential used as the polarization potential is presented in the work of Arretche et al. [32]:

$$V_P(r, r_c) = -\frac{e^2}{2r^4}\left(1 - \exp\left(-\left(\frac{r}{r_c}\right)^6\right)\right), \tag{9}$$

where r_c is the cutoff parameter, determined by fitting it to reproduce previously known experimental or theoretical data. For the e-He interaction, the cutoff parameter is $r_c = 0.526a_0$, and the polarizability of the atom is $\alpha_d = 1.38a_0^3$, with a_0 being the Bohr radius. The cutoff function in Equation (9) reduces the potential at short distances ($r < r_c$), while restoring the asymptotic form $-\frac{\alpha_d}{2r^4}$ for $r > r_c$. This asymptotic form is derived within the framework of the adiabatic approximation, and the given equation accounts for non-adiabatic effects [33,34].

 doi:10.20944/preprints202411.1356.v1

When the incoming particle is an electron, we must also consider rearrangement collisions, where the incoming electron swaps place with an atomic electron. To account for exchange effects, a local exchange potential was used as described by Rosmej et al. [35]. This potential is approximated in the context of a free electron gas [36]:

$$V_{\text{ex}}^{r}(r) = V_{\text{ex}}^{M}[r, K(r)] = -\frac{2}{\pi} K_F(r) F(\eta), \tag{10}$$

where the function $F(\eta)$ is given by:

$$F(\eta) = \frac{1}{2} + \frac{1-\eta^2}{4\eta} \ln\left|\frac{\eta+1}{\eta-1}\right|, \tag{11}$$

and η is defined as the ratio of the momentum of the incoming electron to the maximum momentum corresponding to the surface of the Fermi sphere in momentum space:

$$\eta = \frac{K(r)}{K_F(r)}, \tag{12}$$

where the Fermi wave vector $K_F(r)$ is defined as:

$$K_F(r) = [3\pi^2 \rho(r)]^{1/3}. \tag{13}$$

The value of $K(r)$ is chosen as given by Rosmej et al. [35]:

$$K_{\text{RRR}}^2(r) = k^2 + \frac{2m}{\hbar^2}\Big(|V_{\text{HF}}(r)| + |V_P(r)| + |V_{\text{ex}}^{M}(r,0)|\Big), \tag{14}$$

where

$$V_{\text{ex}}^{M}(r,0) = -\frac{2}{\pi} K_F(r). \tag{15}$$

2.3. Effective Collision Frequency and Energy Transfer Rate

The effective collision frequency $\overline{\nu}_{\text{eff}}$ for an electron interacting with a neutral atom in a Maxwellian plasma is derived from the momentum transfer cross section Q_T^{ea} as follows [22]:

$$\overline{\nu}_{\text{eff}} = \frac{8}{3\sqrt{\pi}} n \left(\frac{m_e}{2k_B T_e}\right)^{5/2} \int_0^\infty v^5 Q_T^{ea}(v) \exp\left(-\frac{m_e v^2}{2kT_e}\right) dv, \tag{16}$$

where v is the electron velocity, k_B is the Boltzmann constant, n is the density of the atoms, and T_e is the electron temperature.

In this equation, the integral captures the contributions of various electron velocities to the effective collision frequency, emphasizing the weight of higher velocities through the v^5 term. The exponential term accounts for the thermal distribution of velocities in the plasma, ensuring that lower velocities have a significantly reduced impact on the effective collision frequency.

Using the effective collision frequency $\overline{\nu}_{\text{eff}}$ from the previous equation, the energy transfer rate can be determined as follows:

$$\frac{dU_e}{dt} = -3n_e \frac{m_e}{m_2} k_B (T_e - T_{He}) \overline{\nu}_{\text{eff}}. \tag{17}$$

where T_{He} and m_{He} are the temperature and mass of the helium atoms.

 doi:10.20944/preprints202411.1356.v1

3. Results and Discussion

3.1. Interaction Potentials

The graphs of the potentials described above are shown in Figure 1. The main contributions to the optical potential are from the polarization potential $V_P(r)$ and the Dirac-Hartree-Fock-Slater potential $V_{DHFS}(r)$. As shown in Figure 1, the behavior of the optical potential tends asymptotically to $-\alpha_d/(2r^4)$ for distances greater than the cutoff parameter r_c in the polarization potential (see Equation (9)). The optical potential has a minimum, which is due to the superposition of the different potentials.

The polarization potential ($V_P(r)$) accounts for the induced dipole moment resulting from the interaction between the electron and the helium atom. The exchange potential ($V_{\text{ex}}(r)$) accounts for the exchange interaction where the incoming electron and one of the atomic electrons exchange places, which becomes significant for low-energy scattering.

The figure illustrates that the optical potential has a well-defined minimum due to the combined effects of the static and polarization components, providing an attractive interaction at certain distances that influence scattering properties.

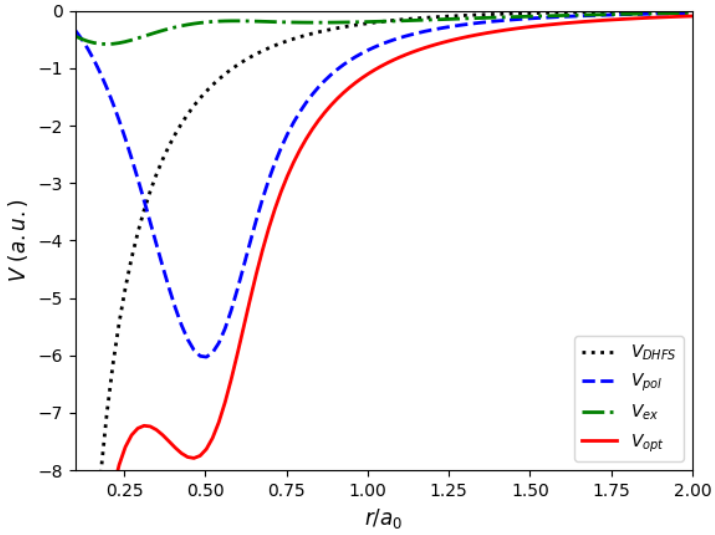

Figure 1. Potential energies of the e-He interaction. The optical potential is represented by a solid line, showing contributions from static (V_{DHFS}), polarization (V_P), and exchange (V_{ex}) potentials.

3.2. Phase Shifts and Momentum Transfer Cross-Sections

The scattering phase shifts, as defined in Equation (3), were calculated based on the optical potential given in Equation (6). Figure 2 shows the results for various angular momentum quantum numbers l as a function of electron energy E. Positive phase shifts ($\delta_l > 0$) indicate an attractive interaction potential. Our results align well with both the theoretical predictions of McEachran et al. [37] and the experimental findings of Williams et al. [38].

For the s-wave, as shown in Figure 2, Levinson's theorem [39] is satisfied, indicating that the scattering phase shift at zero energy is $\delta_l(0) = \pi n$, where n is the number of bound states.

 doi:10.20944/preprints202411.1356.v1

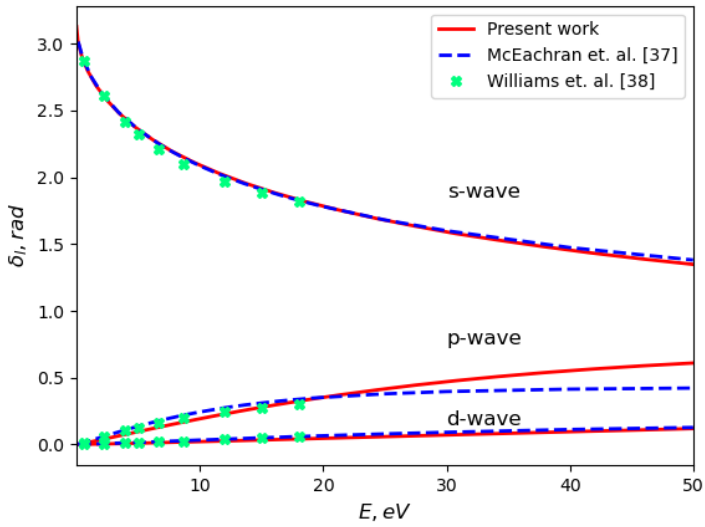

Figure 2. Phase shifts of electron scattering on a helium atom for s-wave ($l = 0$), p-wave ($l = 1$), and d-wave ($l = 2$).

Figure 3 shows the momentum transfer cross sections for electron scattering on a helium atom, compared with theoretical and experimental data from other authors. In our study, we used an optical potential approach similar to that presented in [35,40], where the electron-atom interaction is modelled by combining Coulomb and polarization potentials to account for interactions at short and long distances, respectively. The exchange contribution is represented by an effective local field defined using the static exchange approximation. Our numerical results are in good agreement with experimental data [41–43], as well as with the results of Adibzadeh [44]. The Dirac equation was solved to determine $V_S(r)$ in Adibzadeh's work, whereas we used a model potential, as noted in Equation (2), which allowed us to perform calculations more efficiently without solving complex quantum mechanical equations.

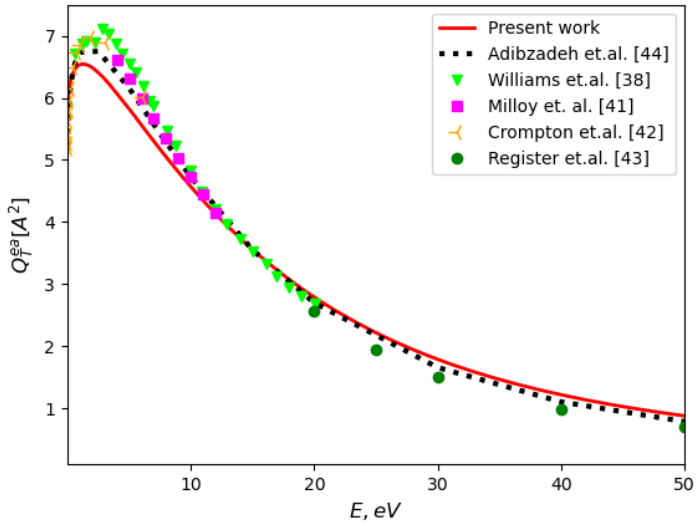

Figure 3. Momentum-transfer cross section of electron scattering on a helium atom.

 doi:10.20944/preprints202411.1356.v1

3.3. Effective Collision Frequency and Energy Transfer Rate

The results of our effective collision frequency calculations are shown in Figure 4, compared with the results from other authors. The use of the momentum transfer cross-section calculated by the optical potential method led to an interesting result. The resulting effective frequency shows a maximum at an energy of approximately 5 eV, which has not been found in other theoretical works that mostly use constant values for the momentum transfer cross-section. Experimental data from Sokolov et al. [45] is consistent with this maximum, and at energies lower than the maximum, our results match well with other theoretical and experimental works [46].

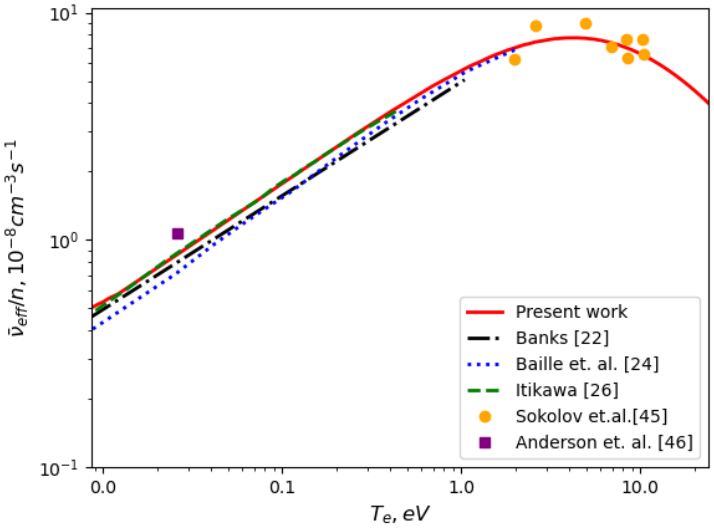

Figure 4. Effective collision frequency between an electron and a helium atom.

The effective collision frequency given by expression (16) exhibits a maximum with increasing electron temperature. This behavior can be explained by a complex interplay between the electron velocity distribution and the momentum-transfer cross-section. With increasing electron temperature T_e, the fraction of fast electrons in the Maxwell distribution also increases. At the same time, the momentum transfer cross-section does not depend on the electron temperature but on the energy of the incident electron. If the Maxwell distribution has a maximum at electron energies corresponding to the region where the cross section increases, a rise in the collision frequency can be observed. However, a further increase in the fraction of fast electrons leads to a decrease in the collision frequency.

Figure 5 shows the dependence of the energy transfer rate on the electron temperature at Helium gas temperature of $T_{He} = 5$ eV. Figures 7 and 8 illustrate the energy transfer over time for electron temperatures of $T_e = 5$ eV and $T_e = 20$ eV, respectively, with $T_{He} = 5$ eV.

In Figure 5, the energy transfer rate shows a gradual increase with electron energy until it reaches a maximum near 5 eV. This behavior can be attributed to an increase in the collision frequency at lower electron energies, which results in the efficient energy transfer between the electrons and helium atoms.

 doi:10.20944/preprints202411.1356.v1

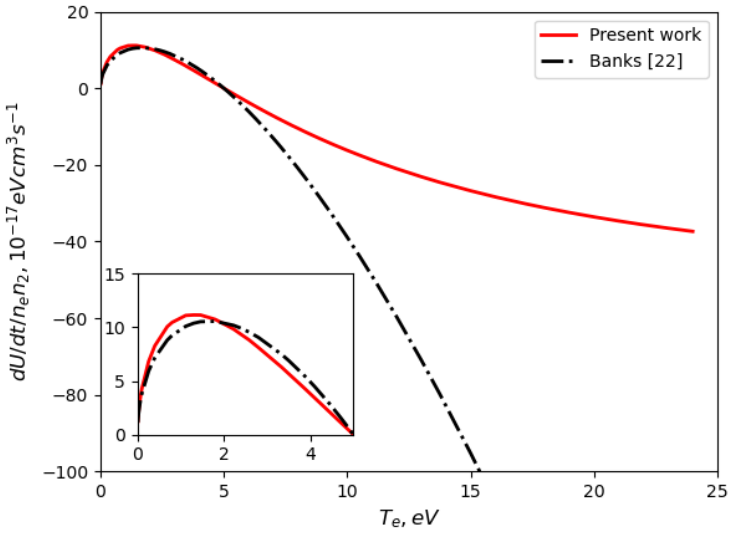

Figure 5. Energy transfer rate between an electron and a helium atom at $T_{He} = 5$ eV.

Figure 6 illustrates the energy transfer rate between electrons and helium atoms, with the rate governed by the relation (17). The energy transfer rate behavior reflects a competition between the electron and helium temperatures. The transfer rate peaks at lower electron temperatures when helium atoms have higher temperatures (which is rather impossible).

As the electron temperature increases beyond the helium temperature, the energy transfer rate diminishes, eventually becoming negative. The negative values indicate that electrons begin to transfer energy to the helium atoms, reversing the direction of energy flow. This crossover occurs because the temperature difference ($T_e - T_{He}$) changes sign, causing a shift in the energy flow direction.

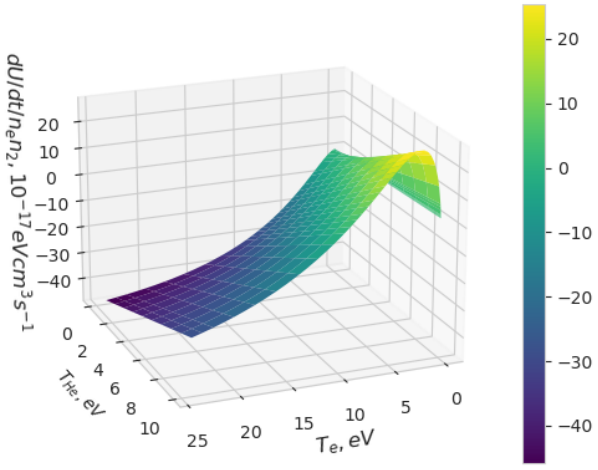

Figure 6. energy transfer rate between electrons and helium atoms as a function of electron and helium temperatures.

Figure 7 illustrates the energy transfer between an electron and a helium atom over time for an electron temperature of $T_e = 5$ eV and a gas atom temperature of $T_{He} = 5$ eV. At this temperature, the energy transfer remains relatively stable over time, indicating that the collision frequency reaches an

 doi:10.20944/preprints202411.1356.v1

optimal value. This results in a consistent energy exchange, which can be beneficial for maintaining equilibrium conditions in plasma.

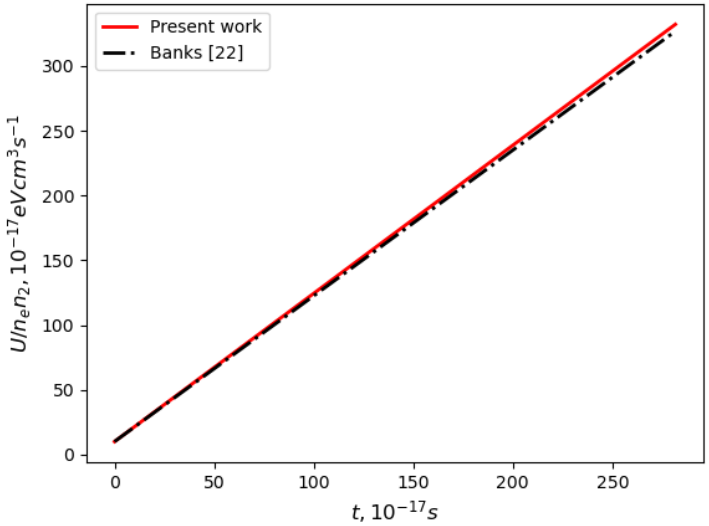

Figure 7. Energy transfer between an electron and a helium atom as a function of time at $T_e = 5$ eV and $T_{He} = 5$ eV.

At a higher electron temperature of $T_e = 20$ eV, as seen in Figure 8, the energy transfer rate decreases significantly compared to the lower temperature cases. This is mainly due to a reduction in the effective collision frequency as the electron energy increases beyond the previously noted maximum. As the effective collisions become less frequent, the energy transfer rate diminishes, resulting in slower temperature equalization between the electrons and helium atoms.

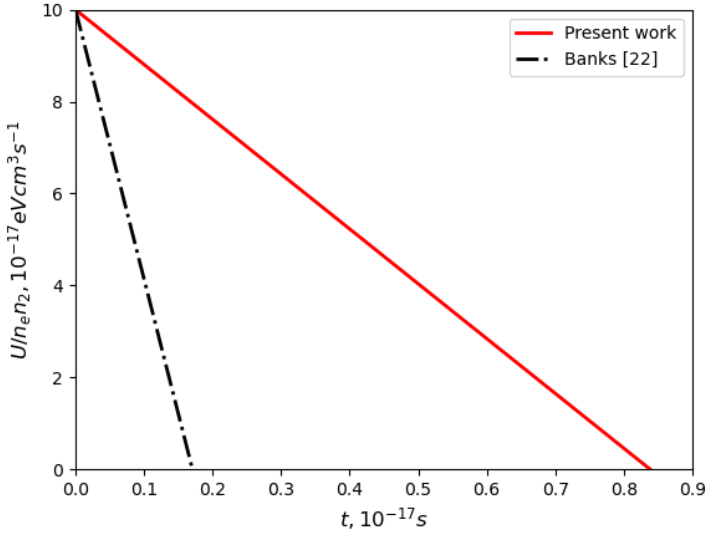

Figure 8. Energy transfer between an electron and a helium atom as a function of time at $T_e = 20$ eV and $T_{He} = 5$ eV.

These results indicate that at higher electron temperatures, the efficiency of energy transfer decreases, which has important implications for plasma behavior in high-temperature environments, such as those found in fusion reactors.

 doi:10.20944/preprints202411.1356.v1

4. Conclusions

The collision frequency and energy transfer rate for electron-helium scattering were determined using the optical potential approach and the phase function method. The results on the collision frequency are consistent with data from other theoretical studies in the field of low electron energies, and at energies above 1 eV, they correspond well with the results obtained in experiments. The presence of a maximum in the collision frequency is a consequence of a decrease in the momentum transfer cross-section with an increase in energy.

At energy values above the detected maximum for the collision frequency, energy transfer calculations indicated that temperature equalization between helium and the electron occurs more slowly. These results are important for determining plasma transport properties such as electron mobility and diffusion coefficients, as well as for calculating electron temperature.

The obtained results can be used in modelling energy exchange processes in the divertor region in Tokamaks. This is an important task, since the processes occurring in the divertor region and even the near-wall region directly affect the processes in the central region of tokamaks and, ultimately, the plasma confinement. In recent studies of electron distribution in tokamaks [47], it has been shown that the electron distribution is often described by the so-called kappa distribution [48,49]. In the Ref. [47] using the kappa distribution resolves discrepancies between experiments and theory based on the use of the Maxwellian distribution function. Since our work shows that considering the Maxwellian velocity distribution and momentum transfer cross-section led to the appearance of the maximum in the dependence of the collision frequency on the electron temperature, at the next stage of our research we plan to consider the effect of the kappa distribution on energy transfer.

Author Contributions: Conceptualization, Yeldos Seitkozhanov; methodology, Yeldos Seitkozhanov and Erik Shalenov; software, Yeldos Seitkozhanov; validation, Yeldos Seitkozhanov, Karlygash Dzhumagulova, and Erik Shalenov; formal analysis, Yeldos Seitkozhanov and Karlygash Dzhumagulova; investigation, Yeldos Seitkozhanov; resources, Yeldos Seitkozhanov; data curation, Yeldos Seitkozhanov; writing - original draft preparation, Yeldos Seitkozhanov; writing - review and editing, Karlygash Dzhumagulova and Yeldos Seitkozhanov; visualization, Yeldos Seitkozhanov; supervision, Murat Jumagulov; project administration, Murat Jumagulov; funding acquisition, Murat Jumagulov. All authors have read and agreed to the published version of the manuscript.

Funding: This research has been funded by the Science Committee of the Ministry of Science and Higher Education of the Republic of Kazakhstan (Grant No. AP19679536).

Conflicts of Interest: The authors declare no conflicts of interest.

References

1. Srivastava, R.; Fursa, D.V. Atoms Special Issue (Electron Scattering from Atoms, Ions, and Molecules). *Atoms* **2023**, *11*, 31.
2. Sahoo, B.K. Constructing Electron-Atom Elastic Scattering Potentials Using Relativistic Coupled-Cluster Theory: A Few Case Studies. *Atoms* **2022**, *10*, 88.
3. Degrave, J.; Felici, F.; Buchli, J.; et al. Magnetic control of tokamak plasmas through deep reinforcement learning. *Nature* **2022**, *602*, 414–419.
4. Trieschmann, J.; Vialetto, L.; Gergs, T. Machine learning for advancing low-temperature plasma modeling and simulation. Available online: https://arxiv.org/abs/2307.00131 (accessed on 5 September 2024).
5. Pines, V.; Pines, M.; Chait, A.; et al. Nuclear fusion reactions in deuterated metals. *Phys. Rev. C* **2020**, *101*, 044609.
6. Zhang, J.; Wang, W.M.; Yang, X.H.; et al. Double-cone ignition scheme for inertial confinement fusion. *Phil. Trans. R. Soc. A* **2020**, *378*, 20200015.
7. Hill, C.; Dipti, K.; Heinola, K.; et al. Atomic collisional data for neutral beam modeling in fusion plasmas. *Nucl. Fusion* **2023**, *63*, 125001.
8. Cichocki, F.; Sciortino, V.; Giordano, F.; Minelli, P.; Taccogna, F. Two-dimensional collisional particle model of the divertor sheath with electron emissive walls. *Nucl. Fusion* **2023**, *63*, 086022.
9. Hesse, M.; Cassak, P.A. Magnetic Reconnection in the Space Sciences: Past, Present, and Future. *J. Geophys. Res. Space Phys.* **2020**, *125*, e2018JA025935.

 doi:10.20944/preprints202411.1356.v1

10. Ripoll, J.-F.; Pierrard, V.; Cunningham, G.S.; et al. Modeling of the Cold Electron Plasma Density for Radiation Belt Physics. *Front. Astron. Space Sci.* **2023**, *10*, 1096595.
11. Blackburn, T.G. Radiation Reaction in Electron-Beam Interactions with High-Intensity Lasers. *Rev. Mod. Plasma Phys.* **2020**, *4*, 5.
12. Gonoskov, A.; Blackburn, T.G.; Marklund, M.; Bulanov, S.S. Charged Particle Motion and Radiation in Strong Electromagnetic Fields. *Rev. Mod. Phys.* **2022**, *94*, 045001.
13. Gelfer, E.G.; Fedotov, A.M.; Klimo, O.; Weber, S. Coherent Radiation of an Electron Bunch Colliding with an Intense Laser Pulse. *Phys. Rev. Res.* **2024**, *6*, L032013.
14. Krüger, K.; Wang, Y.; Tödter, S.; et al. Hydrogen Atom Collisions with a Semiconductor Efficiently Promote Electrons to the Conduction Band. *Nat. Chem.* **2023**, *15*, 326–331.
15. Fletcher, J.D.; Park, W.; Ryu, S.; et al. Time-Resolved Coulomb Collision of Single Electrons. *Nat. Nanotechnol.* **2023**, *18*, 727–732.
16. Knapen, S.; Kozaczuk, J.; Lin, T. Migdal Effect in Semiconductors. *Phys. Rev. Lett.* **2021**, *127*, 081805.
17. Howell, R.W. Advancements in the Use of Auger Electrons in Science and Medicine During the Period 2015–2019. *Int. J. Radiat. Biol.* **2023**, *99*, 2–27.
18. Choi, E.H.; Kaushik, N.K.; Hong, Y.J.; et al. Plasma Bioscience for Medicine, Agriculture and Hygiene Applications. *J. Korean Phys. Soc.* **2022**, *80*, 817–851.
19. Kheradmand Saadi, M.; Machrafi, R. Development of a New Code for Stopping Power and CSDA Range Calculation of Incident Charged Particles, Part A: Electron and Positron. *Appl. Radiat. Isot.* **2020**, *161*, 109145.
20. Dalgarno, A.; Walker, J.C.G. Ion temperatures in the topside ionosphere. *Planetary and Space Science* **1967**, *15*, 200–203.
21. Geisler, J.E. Ionospheric D-Region Absorption in a Proton Flare. *J. Geophys. Res.* **1965**, *70*, 1250–1255.
22. Banks, P.M. Collision Frequencies and Energy Transfer in Aeronomy. *Planet. Space Sci.* **1966**, *14*, 1105–1122.
23. Schunk, R.W.; Walker, J.C.G. Transport Properties of the Ionosphere and Exosphere. *Planet. Space Sci.* **1970**, *18*, 1703–1729.
24. Baille, P.; Chang, J.-S.; Claude, A.; Hobson, R.M.; Ogram, G.L.; Yau, A.W. Effective Collision Frequency of Electrons in Noble Gases. *J. Phys. B: At. Mol. Phys.* **1981**, *14*, 1485–1495.
25. Desloge, E.A. Energy Exchange between Different Species in a Gaseous Mixture. *J. Chem. Phys.* **1962**, *36*, 2431–2435.
26. Itikawa, Y. Effective Collision Frequency for Energy Transfer between Electrons and Neutral Atoms. *J. Phys. Soc. Jpn.* **1971**, *30*, 1296–1300.
27. Babikov, V.V. The Phase Function Method in Quantum Scattering Theory. *Sov. Phys. Usp.* **1967**, *10*, 271–286.
28. Calogero, F. A novel approach to elementary scattering theory. *Il Nuovo Cimento (1955-1965)* **1963**, *27*, 261–302.
29. Dzhumagulova, K.N.; Shalenov, E.O.; Ramazanov, T.S. Elastic scattering of low energy electrons in partially ionized dense semiclassical plasma. *Phys. Plasmas* **2015**, *22*, 082120. https://doi.org/10.1063/1.4928877.
30. Shalenov, E.O.; Seisembayeva, M.M.; Dzhumagulova, K.N.; Ramazanov, T.S. Kinetic ionization and recombination coefficients in the dense semiclassical plasmas on the basis of the effective interaction potential. *J. Phys.: Conf. Ser.* **2019**, *1400*, 077035.
31. Salvat, F.; Mayol, R. Analytical Potentials for Electron and Positron Elastic Scattering by Atoms. *Phys. Rev. A* **1987**, *36*, 467–474.
32. Arretche, F.; Barp, M.V.; Scheidt, A.; Popovicz Seidel, E.; Tenfen, W. Corrigendum: Semiempirical models for low energy positron scattering by Ar, Kr and Xe. *J. Phys. B: At. Mol. Opt. Phys.* **2020**, *53*, 209501.
33. Mitroy, J.; Bromley, M.W.J.; Zhang, J.Y. Semiempirical Exchange Potentials for Electron Scattering from Atoms. *Phys. Rev. A* **2002**, *65*, 032507.
34. Kunc, J.A. Low-Energy Electron-Atom Scattering in a Field of Model Potentials. *J. Phys. B At. Mol. Opt. Phys.* **1999**, *32*, 607–619.
35. Rosmej, S.; Reinholz, H.; Röpke, G. Contribution of Electron-Atom Collisions to the Plasma Conductivity of Noble Gases. *Phys. Rev. E* **2017**, *95*, 063208.
36. Mittleman, M.H.; Watson, K.M. Effects of the Pauli Principle on the Scattering of High-Energy Electrons by Atoms. *Ann. Phys.* **1960**, *10*, 268–279.
37. McEachran, R.P.; Stauffer, A.D. Polarisation and Exchange Effects on Elastic Scattering of Electrons from Helium. *J. Phys. B: At. Mol. Phys.* **1983**, *16*, 25.

 doi:10.20944/preprints202411.1356.v1

38. Williams, J.F. A Phase Shift Analysis of Experimental Angular Distributions of Electrons Elastically Scattered from He, Ne, and Ar over the Range 0.5 to 20 eV. *J. Phys. B: At. Mol. Phys.* **1979**, *12*, 265.
39. Wellner, M. Levinson's Theorem (an Elementary Derivation). *Am. J. Phys.* **1964**, *32*, 787–789.
40. Dzhumagulova, K.N.; Shalenov, E.O.; Tashkenbayev, Y.A.; Ramazanov, T.S. Study of the electron–atom collisions in dense semiclassical plasma of noble gases. *J. Plasma Phys.* **2022**, *88*, 905880119.
41. Milloy, H.B.; Crompton, R.W. Momentum-transfer cross section for electron-helium collisions in the range 4-12 eV. *Phys. Rev. A* **1977**, *15*, 1847–1850.
42. Crompton, R.W.; Elford, M.T.; Robertson, A.G. The momentum transfer cross section for electrons in helium derived from drift velocities at 77K. *Aust. J. Phys.* **1970**, *23*, 667.
43. Register, D.F.; Trajmar, S.; Srivastava, S.K. Absolute elastic differential electron scattering cross sections for He: A proposed calibration standard from 5 to 200 eV. *Phys. Rev. A* **1980**, *21*, 1134–1151.
44. Adibzadeh, M.; Theodosiou, C.E. Elastic Electron Scattering from Inert-Gas Atoms. *At. Data Nucl. Data Tables* **2005**, *91*, 8–76.
45. Sokolov, V.F.; Sokolova, Y.A.; Khalimulina, V.D. Frequency of Collisions between Electrons and Gas and Vapor Atoms and Molecules. *Sov. Phys. J.* **1983**, *26*, 869–873.
46. Anderson, J.M.; Goldstein, L. Interaction of Electromagnetic Waves of Radio-Frequency in Isothermal Plasmas: Collision Cross Section of Helium Atoms and Ions for Electrons. *Phys. Rev.* **1955**, *100*, 1037–1046.
47. Dumont, R. J.; Phillips, C. K.; Smithe, D. N. Effects of non-Maxwellian species on ion cyclotron waves propagation and absorption in magnetically confined plasmas. *Physics of Plasmas* **2005**, *12*, 042508.
48. Livadiotis, G. *Kappa Distributions: Theory and Applications in Plasmas*; Elsevier: Amsterdam, 2017; pp. 1–724.
49. Rubab, N.; Murtaza, G. Debye length in non-Maxwellian plasmas. *Physica Scripta* **2006**, *74*, 145.